

## Selective excitation of $E_1(\text{LO})$ and $A_1(\text{LO})$ phonons with large wave vectors in the Raman spectra of hexagonal InN

V. Yu. Davydov,<sup>1,\*</sup> A. A. Klochikhin,<sup>1,2</sup> A. N. Smirnov,<sup>1</sup> I. Yu. Strashkova,<sup>1</sup> A. S. Krylov,<sup>3</sup> Hai Lu,<sup>4</sup> William J. Schaff,<sup>4</sup> H.-M. Lee,<sup>5</sup> Y.-L. Hong,<sup>5</sup> and S. Gwo<sup>5</sup>

<sup>1</sup>*Ioffe Physical-Technical Institute, 194021 St. Petersburg, Russia*

<sup>2</sup>*Nuclear Physics Institute, 350000 St. Petersburg, Russia*

<sup>3</sup>*Kirensky Institute of Physics, 660036 Krasnoyarsk, Russia*

<sup>4</sup>*Department of Electrical and Computer Engineering, Cornell University, Ithaca, New York 14853, USA*

<sup>5</sup>*Department of Physics, National Tsing-Hua University, Hsinchu 30013, Taiwan, Republic of China*

(Received 16 July 2009; published 27 August 2009)

It is shown that dispersions of  $E_1(\text{LO})$  and  $A_1(\text{LO})$  modes of InN can be restored in a wide interval of wave vectors by studying impurity-induced first-order Raman scattering as a function of exciting light energy. It is also shown that due to the resonance character of scattering the observed phonon energies correspond to the wave vectors strictly defined by exciting photon energies. The frequencies of  $E_1(\text{LO})$  and  $A_1(\text{LO})$  phonons at the  $\Gamma$  point obtained by extrapolation to zero wave vectors were found to be 604 and 592  $\text{cm}^{-1}$ , respectively.

DOI: 10.1103/PhysRevB.80.081204

PACS number(s): 78.30.Fs, 71.20.Nr, 63.20.dd

Energies of longitudinal phonons (LO) at the  $\Gamma$  point are among fundamental characteristics of vibrational spectrum of a crystal, however, for InN available data are still controversial. A narrow line at 586–591  $\text{cm}^{-1}$  the position of which varies only slightly as the electron concentration changes in wide limits was detected in Raman spectra of hexagonal InN. This line was ascribed to the  $A_1(\text{LO})$  mode with large wave vectors resulting from violation of the wave-vector conservation law.<sup>1–3</sup> The agreement between theoretical considerations and experimental data was achieved in these papers when the wave vectors became larger than the upper Landau damping boundary<sup>2</sup> or essentially large than the Thomas-Fermi wave vector.<sup>3</sup> No analysis of the behavior of  $E_1(\text{LO})$  phonon is available in literature to our knowledge. There are also data indicating that frequencies of  $A_1(\text{LO})$  phonon<sup>4,5</sup> and  $E_1(\text{LO})$  phonon<sup>5</sup> in hexagonal InN vary as excitation energy changes. However, no studies of this effect have been carried out so far.

This Rapid Communication reports on a systematic investigation of dependences of  $E_1(\text{LO})$  and  $A_1(\text{LO})$  phonon frequencies on exciting photon energy. It is shown that changes in the LO frequencies are related to the dispersions of these modes. The changes arise due to strict selection of wave vectors by the energy conservation laws in the intermediate states of the resonant scattering amplitude. We report also that the polar acoustic phonons with large wave vectors selected by the resonant amplitude are active in the Raman spectra.

The parameters of MBE-grown undoped and Mg-doped InN samples<sup>6,7</sup> used in our studies are given in Table I. Room-temperature Raman spectra for excitation energies from 2.81 to 1.83 eV were measured with a Jobin-Yvon Horiba T64000 triple Raman spectrometer with a confocal microscope. Measurements with an excitation energy of 1.17 eV were carried out with a Bruker RFS100/S Raman Fourier spectrometer. All spectra were measured in backscattering geometry. Scattering from the cleavage plane and surface side of the high-quality thick undoped InN (Gs2054) sample was used to obtain data on  $E_1(\text{LO})$  and  $A_1(\text{LO})$  phonons at excitation in the 2.81–1.83 eV range. When an energy of

1.17 eV is used for excitation, measurements of Raman spectrum of undoped InN are hindered by an intense interband luminescence. To solve the problem, we studied Mg-doped InN samples in which luminescence was suppressed at room temperature and Raman spectrum was reliably detected. The  $E_1(\text{LO})$  phonon was measured on the  $a$ -InN:Mg sample grown on a  $r$ -plane  $\text{Al}_2\text{O}_3$ . Its hexagonal axis was parallel to the substrate plane and had a fixed orientation. The  $A_1(\text{LO})$  phonon was measured on the InN:Mg sample grown on a  $c$  plane  $\text{Al}_2\text{O}_3$  the hexagonal axis of which was normal to the substrate plane.

Figure 1 presents polarized Raman spectra of undoped InN in the region of optical phonons. The spectra are normalized to the  $A_1(\text{TO})$  or  $E_2(\text{high})$  mode intensity and shifted along the vertical axis. It can be seen that the  $A_1(\text{TO})$  and  $E_2(\text{high})$  mode positions at 449.0 and 491.5  $\text{cm}^{-1}$ , respectively, does not change as excitation energy varies. However, both LO phonon lines experience high-frequency shifts and intensity growth with decreasing excitation energy. For example, at 2.81 eV, the  $E_1(\text{LO})$  and  $A_1(\text{LO})$  phonon frequencies are 591.0 and 580.5  $\text{cm}^{-1}$ , respectively. As the excitation energy is decreased to 1.83 eV, the  $E_1(\text{LO})$  and  $A_1(\text{LO})$  mode frequencies become 599.0 and 587.5  $\text{cm}^{-1}$ , respectively.

The inset to Fig. 1(a) shows Raman spectra for the  $a$ -InN:Mg sample grown on  $r$ -plane sapphire substrate. As measurements with excitation energies from 2.81 to 1.83 eV showed, slight doping with Mg does not affect the linewidth and position of the maximum of the  $E_1(\text{LO})$  phonon. So, it can be inferred that the Raman spectrum measured on  $a$ -InN:Mg can be used to estimate the  $E_1(\text{LO})$  phonon fre-

TABLE I. Parameters of InN samples.

Sample	InN layer	$n_e$ ( $\text{cm}^{-3}$ )	$n_{\text{Mg}}$ ( $\text{cm}^{-3}$ )	Thickness ( $\mu\text{m}$ )
Gs2054	InN	$3.5 \times 10^{17}$		5.5
071125	$a$ -InN:Mg	$2.8 \times 10^{18}$	$2 \times 10^{18}$	1.3
Gs1810	InN:Mg	$1.9 \times 10^{18}$	$6 \times 10^{18}$	0.5

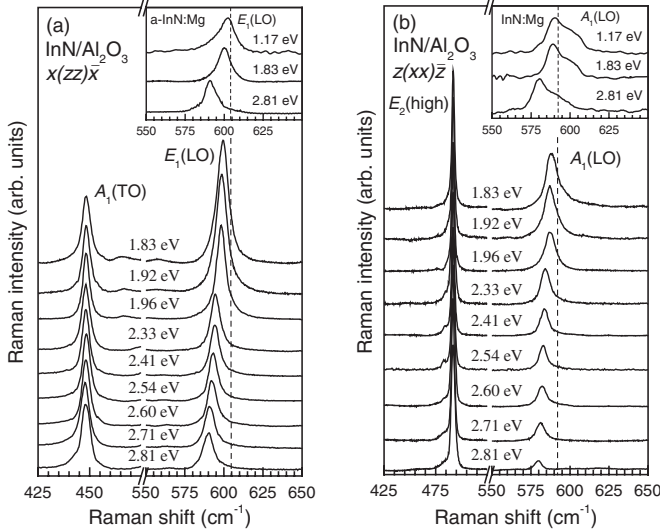


FIG. 1. Room-temperature polarized Raman spectra of  $E_1(\text{LO})$  and  $A_1(\text{LO})$  modes of hexagonal InN obtained in  $x(\text{zz})\bar{x}$  and  $z(\text{xx})\bar{z}$  scattering configurations for different excitation energies. Here,  $z$  is the InN hexagonal axis direction. The dashed lines show estimated LO phonon frequencies at the  $\Gamma$  point.

quency at 1.17 eV excitation which was found to be  $602.0 \text{ cm}^{-1}$ .

The inset to Fig. 1(b) shows Raman spectra for the InN:Mg sample grown on a  $c$ -plane sapphire substrate. The Mg concentration in this sample is higher than that in  $a$ -InN:Mg. It can be seen that a shoulder on the high-frequency side of the  $A_1(\text{LO})$  phonon line appears in the InN:Mg spectrum. We assign this feature to the forbidden  $E_1(\text{LO})$  mode caused by defect-induced relaxation of selection rules. However, it has been found that the position of the  $A_1(\text{LO})$  band maximum is the same for InN:Mg and undoped InN sample for excitation in the 2.81–1.83 eV range. This finding allows estimation of the  $A_1(\text{LO})$  phonon frequency at the 1.17 eV excitation by using the InN:Mg sample which was found to be  $590.5 \text{ cm}^{-1}$ .

The peculiarities of the electron band structure of InN play an important role in the forming of the Raman-scattering process. The direct electromagnetic transitions from valence bands occur in a wide energy interval to the single conduction band with the extremum at the  $\Gamma$  point.<sup>8</sup> This means that the Martin's double resonance<sup>9,10</sup> is realized in a wide interval of the excitation photon energies.

The first-order Raman scattering from LO phonons taking into account the wave-vector conservation law violation due to scattering of electrons and holes from charged impurity centers is described in the forth order of the perturbation theory. The corresponding scattering amplitude contains two electromagnetic interactions  $H_{em}$  and  $H'_{em}$ , the Fröhlich interaction of the photoexcited electron-hole pair with the phonon  $H_{int}$ , and the Coulomb interaction with charged impurity centers  $H_i$ ,

$$A \propto \left\{ \sum_{\lambda, \lambda'} \frac{[H_{em}]_{0, \lambda} [H_{int}]_{\lambda, \lambda'} [H_i]_{\lambda', \lambda''} [H'_{em}]_{\lambda'', 0}}{\hbar^3 (\omega - \Omega_{\lambda, 0}) (\omega' - \Omega_{\lambda', 0}) (\omega' - \Omega_{\lambda'', 0})} \right\}. \quad (1)$$

Here,  $\omega$  and  $\omega'$  are the frequencies of incident and scattered photons, and  $\Omega_{\lambda, 0}$ ,  $\Omega_{\lambda', 0}$ , and  $\Omega_{\lambda'', 0}$  are the frequencies of

interband transitions. If the exciting (and scattered) photon energy exceeds the absorption threshold, the process becomes resonant in the sense that the virtual intermediate states of the scattering amplitude become real. The Fröhlich and Coulomb intraband interactions are the most effective in processes of the photoexcited pair relaxation. This leads to a higher Raman-scattering probability and to restrictions on the magnitudes of phonon wave vectors arising during scattering.

A strong dependence of the amplitude on the phonon wave vector arises, similar to 2LO scattering amplitude,<sup>11</sup> from denominators of Eq. (1) which can take zero value if scattering occurs in the region of interband absorption. Let us write the scattering amplitude neglecting the photon wave-vector magnitudes and preserving only the denominators that play a crucial role in the dependence on the phonon wave vector

$$A(q, \omega) \propto \iiint \frac{d^3 p d^3 p_1 d^3 p_2}{(\omega - \Omega_p^{eh}) (\omega' - \Omega_{p_2}^{eh}) (\omega_1 - \Omega_{p_1}^{eh} - \hbar q^2 / 2M)} \times (\delta(\mathbf{p} - \mathbf{p}_1 + \mathbf{q}^e) - \delta(\mathbf{p} - \mathbf{p}_1 + \mathbf{q}^h)) \times (\delta(\mathbf{p}_1 - \mathbf{p}_2 + \mathbf{q}^e) - \delta(\mathbf{p}_1 - \mathbf{p}_2 + \mathbf{q}^h)), \quad (2)$$

where  $\Omega_p^{eh} = E_g / \hbar + \hbar p^2 / 2\mu$ ,  $E_g$  is the band-gap width,  $\mu = m_e^* m_h^* / (m_e^* + m_h^*)$  is the reduced effective mass of electron and hole,  $M$  is the translational mass of the pair,  $q^{e,h} = q\mu / m_{e,h}^*$  and  $\hbar^2 p^2 / 2\mu$  is kinetic energy of relative motion of the electron-hole pair. The amplitude contains two terms, in the first one  $\omega_1 = \omega$ , and in the second term  $\omega_1 = \omega'$ , and we consider in detail one of them.

The  $\delta$  functions allows us to integrate over  $d^3 p_1$  and  $d^3 p_2$ . Integrating over angular variables of vector  $\mathbf{p}$  we present the real and imaginary parts of the denominator as  $\frac{1}{(\Delta - (\hbar^2 p^2 / 2\mu) - i\delta)} = \frac{1}{(\Delta - (\hbar^2 p^2 / 2\mu)_p} + i\pi \delta(\Delta - \frac{\hbar^2 p^2}{2\mu})$ , where  $\Delta = \hbar\omega - E_g$ . Similarly we treat the denominator containing  $\Delta' = \hbar\omega' - E_g$ . Now we can integrate over  $dp^2$  by using  $\delta$ -function that expresses the energy conservation laws at electromagnetic transitions. This means that we consider the scattering process involving real absorption or real emission. The contribution into the scattering amplitude due to real electromagnetic transitions is given by

$$A(q, \omega) \propto \left[ \frac{2\mu(m_e + m_h)v_0}{(2\pi)^2 \hbar^2 q} \right] \frac{2\mu}{\hbar(p_\omega + p_{\omega'})} \times \left[ \frac{p_\omega}{(p_\omega^2 - q^2/4 - i\mu\gamma/\hbar)} + \frac{p_{\omega'}}{(p_{\omega'}^2 - q^2/4 - i\mu\gamma/\hbar)} \right]. \quad (3)$$

Here,  $p_\omega = \sqrt{2\mu\Delta/\hbar^2}$  and  $p_{\omega'} = \sqrt{2\mu\Delta'/\hbar^2}$ . The scattering cross section which is proportional to the square of amplitude modulus of Eq. (3) will determine the phonon wave vectors  $q$  by relating their values to the exciting or scattered light frequency by equations  $q = 2p_\omega$  or  $q = 2p_{\omega'}$ . The uncertainty of these values is defined by the relaxation time of the electron-hole pair  $\tau$  which is related to the intermediate-state broadening  $\gamma$  by equation  $\gamma = 1/\tau$ . Therefore, the phonon

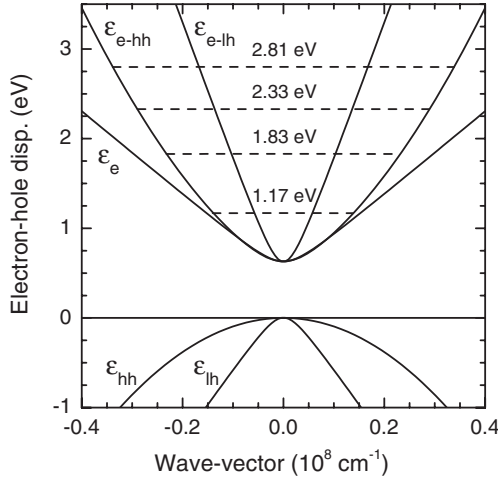


FIG. 2. Dispersions of valence bands, conduction band, and electron-hole pairs of hexagonal InN. The dashed lines correspond to excitation photon energies.

wave-vector magnitudes following from the energy conservation laws in the intermediate states are  $q=2p_\omega \pm \sqrt{2\mu\gamma/\hbar}$  and  $q=2p_\omega \pm \sqrt{2\mu\gamma/\hbar}$ . Thus, the interval of phonon wave vectors increases as the electron-hole pair damping grows. The accuracy of phonon wave-vector magnitude depends also on the correctness of the electron band parameters.

Finally, by integrating over  $dq^2$ , we obtain for the Raman cross section due to Fröhlich interaction and scattering of the electron-hole pair from charged impurities

$$\sigma(\omega) \propto \frac{N_i}{2\pi^2} \frac{p_\omega}{(p_\omega + p_\omega')^2} \left| \frac{4\pi Ze}{v_c \epsilon_\infty (4p_\omega^2 + q_{TF}^2)} \right|^2 \frac{1}{\mu\gamma/\hbar} \frac{2\pi}{\hbar} \times \delta[\omega - \omega' - \Omega_{\text{LO}}(q = 2p_\omega)]. \quad (4)$$

Here,  $N_i$  and  $Z$  are the impurity center concentration and charge, respectively,  $v_c$  is the volume of the elementary cell, and  $q_{TF}$  is the Thomas-Fermi screening wave vector. A similar contribution arises from the second term of the amplitude given by Eq. (2) and can be obtained from Eq. (4) by substituting  $p_\omega \rightleftharpoons p_\omega'$ . As long as the  $q$  values are above the upper boundary of Landau damping, i.e., as long as  $2p_\omega > 2p_F + \sqrt{2m^* \Omega_{\text{LO}}/\hbar}$ , the scattering results in a unscreened phonon of the longitudinal optical branch. This kind of cross section is typical of InN samples with moderate electron concentrations.

The phonon wave-vector magnitude depends on electron-hole pair dispersion. The data on InN photoemission<sup>12,13</sup> allows one to find dispersions of conduction, light hole, and heavy-hole bands. Figure 2 shows dispersions of these bands and electron-hole pairs arising at direct transitions from the heavy (E-HH) and light (E-LH) hole bands into the conduction band. The nonparabolic dispersion of the electron band, as shown in Ref. 14, is well described by the expression  $\epsilon^e(k) = E_e \sqrt{\hbar^2 k^2 / 2m_\Gamma^e E_e + 1/4 - 1/2}$ , which corresponds to a linear increase in the effective mass with kinetic energy. Here,  $m_\Gamma^e$  is the effective electron mass at the  $\Gamma$  point ( $m_\Gamma^e = 0.07m_0$ ) and  $E_e$  is the nonparabolicity parameter ( $E_e = 0.4$  eV). A similar expression was used for the light hole

band dispersion  $\epsilon^{lh}(k) = -E_{lh} \sqrt{\hbar^2 k^2 / 2m_\Gamma^{lh} E_{lh} + 1/4 - 1/2}$ , where  $m_\Gamma^{lh}$  is the effective mass of a light hole at the  $\Gamma$  point ( $m_\Gamma^{lh} = 0.035m_0$ ) and  $E_{lh}$  is the nonparabolicity parameter ( $E_{lh} = 0.8$  eV). For the heavy-hole band the parabolic approximation with  $m^{hh} = 0.4m_0$  was used. For plotting Fig. 2, the band gap at room temperature was taken to be 0.63 eV. The phonon wave-vector magnitudes correspond to the doubled wave vectors at which the horizontal line at the exciting photon energy intersects the dispersion curves of electron-hole pairs. As can be seen from Fig. 2 these magnitudes markedly differ for the E-HH and E-LH pairs. The analysis given below is devoted to the question how these transitions can be related with the observed phonons.

As can be seen in Fig. 1(b), the  $A_1(\text{LO})$  line monotonically shifts toward lower frequencies as the exciting photon energy increases from 1.17 to 2.81 eV. This corresponds to variations in the phonon wave vector from 0.115 to  $0.335 \times 10^8 \text{ cm}^{-1}$  if E-LH transitions occur and from 0.28 to  $0.68 \times 10^8 \text{ cm}^{-1}$  if heavy holes participate in transitions. The  $A_1(\text{LO})$  branch exists only in  $\Gamma$ -A direction and its frequency decreases from a maximum at the  $\Gamma$  point to a minimum at the Brillouin-zone boundary.<sup>15</sup> The limiting value of the wave vector at the Brillouin-zone boundary is  $0.55 \times 10^8 \text{ cm}^{-1}$ . Thus, the observed monotonic frequency decrease with increasing wave vector is possible only if the wave-vector magnitude does not exceed the boundary value. This is fulfilled for the E-LH transitions and is not fulfilled for the E-HH transitions. Therefore, only the E-LH transitions in the Raman-scattering amplitude are accompanied by the  $A_1(\text{LO})$  phonon excitation.

The upper panel of Fig. 3 shows dispersion of the  $A_1(\text{LO})$  branch plotted in the wave-vector intervals corresponding to E-LH and the  $E_1(\text{LO})$  branch corresponding to E-HH transitions. For the samples studied and for the exciting photon energies used, the minimal values of the phonon wave vectors are above the upper boundary of Landau damping, which, with due account for conduction-band nonparabolicity, is  $0.080$  and  $0.111 \times 10^8 \text{ cm}^{-1}$  for electron concentrations  $3.5 \times 10^{17}$  and  $2.0 \times 10^{18} \text{ cm}^{-3}$ , respectively. Only the uncoupled LO phonons exist above this boundary. The extrapolation of the dispersions of LO modes gives the frequencies of these phonons at  $\Gamma$  point.

The lower panel of Fig. 3 shows the calculated dispersion curves of InN taken from Ref. 15 and experimental data on the  $A_1(\text{LO})$  frequencies plotted along  $\Gamma$ -A direction as well as  $E_1(\text{LO})$  frequencies plotted along  $\Gamma$ -M direction. It can be seen that the experiment and theory are in satisfactory agreement.

Figure 4 presents polarized Raman spectra sample Gs2054 in the region of acoustic phonons obtained with excitation energies from 2.71 to 1.83 eV. It is seen that the frequency of the line changes by about  $45 \text{ cm}^{-1}$  within the excitation energy interval. This behavior of phonons can be understood if we assume that Raman scattering from LA phonons involves electromagnetic E-HH transitions. The wave vectors corresponding to the excitation energies used occupy the  $0.46$ – $0.66 \times 10^8 \text{ cm}^{-1}$  interval. As seen in the lower panel of Fig. 3 the experimental acoustic phonon frequencies are consistent with the calculated ones for the LA branch along the  $\Gamma$ -M direction (according to our estimates

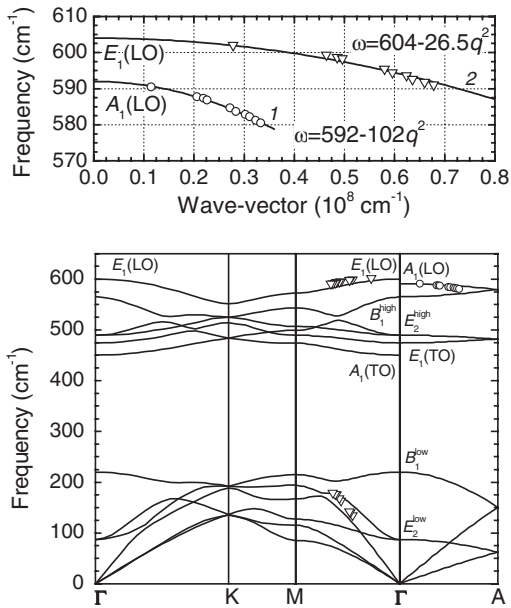


FIG. 3. Top panel: frequencies of  $A_1(\text{LO})$  and  $E_1(\text{LO})$  phonons as a function of phonon wave vectors  $q=2p_\omega$ . The wave vectors are calculated for E-LH (curve 1) and E-HH (curve 2) transitions. The symbols are experimental frequencies. The solid lines are dispersion approximations of  $A_1(\text{LO})$  and  $E_1(\text{LO})$  branches by parabolic curves. Lower panel: InN phonon-dispersion curves taken from Ref. 15 and experimental data of this work (symbols).

the acoustic wave velocity is  $5.43 \times 10^5$  cm/s). However, additional studies are needed to obtain more detail pattern of acoustic phonon scattering.

To summarize, we have found that resonant Raman scattering can excite selectively uncoupled LO as well as LA phonons with large wave vectors. As a result, the dispersions of LO and LA phonon modes of hexagonal InN in the wide

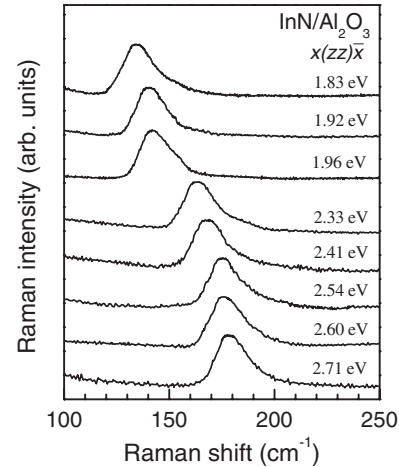


FIG. 4. Room-temperature polarized Raman spectra of hexagonal InN in the region of acoustic phonons obtained in  $x(zz)\bar{x}$  scattering configuration for different excitation energies. Here,  $z$  is the InN hexagonal axis direction. The spectra are normalized to the Raman line maximum.

range of wave vectors have been reconstructed from experimental data. The extrapolation of the  $E_1(\text{LO})$  and  $A_1(\text{LO})$  phonon dispersions to zero wave vectors allowed us to estimate the  $\Gamma$  point energies of these branches that have not been firmly established so far. The data obtained can be useful for the future calculations of the InN lattice dynamics.

We are thankful to B. N. Mavrin and A. N. Vtyurin for the arrangement NIR measurements and S. A. Permogorov for the critical reading of the manuscript. This work was supported by RFBR (Grant No. 09-02-01280), NSC-RFBR (Grant No. 08-02-92003-HHC), and the Program of RAS “New materials and structures.”

\*valery.davydov@mail.ioffe.ru

<sup>1</sup>A. Kasic, M. Schubert, Y. Saito, Y. Nanishi, and G. Wagner, Phys. Rev. B **65**, 115206 (2002).

<sup>2</sup>J. S. Thakur, D. Haddad, V. M. Naik, R. Naik, G. W. Auner, H. Lu, and W. J. Schaff, Phys. Rev. B **71**, 115203 (2005).

<sup>3</sup>F. Demangeot, C. Pinquier, J. Frandon, M. Gaio, O. Briot, B. Maleyre, S. Ruffenach, and B. Gil, Phys. Rev. B **71**, 104305 (2005).

<sup>4</sup>R. Cuscó, J. Ibáñez, E. Alarcón-Lladó, L. Artús, T. Yamaguchi, and Y. Nanishi, Phys. Rev. B **79**, 155210 (2009).

<sup>5</sup>V. Yu. Davydov and A. A. Klochikhin, in *Indium Nitride and Related Alloys*, edited by T. D. Veal, C. F. McConville, and W. J. Schaff (CRC Press, Boca Raton, 2009), p. 208.

<sup>6</sup>H. Lu, W. J. Schaff, J. Hwang, H. Wu, W. Yeo, A. Pharkya, and L. F. Eastman, Appl. Phys. Lett. **77**, 2548 (2000).

<sup>7</sup>Y.-M. Chang, Y.-L. Hong, and S. Gwo, Appl. Phys. Lett. **93**, 131106 (2008).

<sup>8</sup>F. Bechstedt and J. Furthmüller, J. Cryst. Growth **246**, 315

(2002).

<sup>9</sup>R. M. Martin, Phys. Rev. B **10**, 2620 (1974).

<sup>10</sup>J. Menendez and M. Cardona, Phys. Rev. B **31**, 3696 (1985).

<sup>11</sup>A. A. Abdumalikov and A. A. Klochikhin, Phys. Status Solidi B **80**, 43 (1977).

<sup>12</sup>L. Colakerol, T. D. Veal, H.-K. Jeong, L. Plucinski, A. DeMasi, T. Learmonth, P.-A. Glans, S. Wang, Yu. Zhang, L. F. J. Piper, P. H. Jefferson, A. Fedorov, T.-C. Chen, T. D. Moustakas, C. F. McConville, and K. E. Smith, Phys. Rev. Lett. **97**, 237601 (2006).

<sup>13</sup>L. Colakerol, L. F. J. Piper, A. Fedorov, T. C. Chen, T. D. Moustakas, and K. E. Smith, EPL **83**, 47003 (2008).

<sup>14</sup>A. A. Klochikhin, V. Yu. Davydov, I. Yu. Strashkova, and S. Gwo, Phys. Rev. B **76**, 235325 (2007).

<sup>15</sup>V. Yu. Davydov, V. V. Emtsev, I. N. Goncharuk, A. N. Smirnov, V. D. Petrikov, V. V. Mamutin, V. A. Vekshin, S. V. Ivanov, M. B. Smirnov, and T. Inushima, Appl. Phys. Lett. **75**, 3297 (1999).